Different impact of suspended Al_2O_3 nanoparticles on microbial communities: formation of 2D-networks (without humic acids) or 3D-colonies (with humic acids)

Damián Rodríguez Sartori
INIFTA: Instituto de Investigaciones Fisicoquimicas Teoricas y Aplicadas
Alejandro Miñán
INIFTA: Instituto de Investigaciones Fisicoquimicas Teoricas y Aplicadas
Mónica Gonzalez
INIFTA: Instituto de Investigaciones Fisicoquimicas Teoricas y Aplicadas
Mónica Fernández Lorenzo de Mele (mmele@inifta.unlp.edu.ar)
INIFTA: Instituto de Investigaciones Fisicoquimicas Teoricas y Aplicadas https://orcid.org/0000-0002-8093-7551

Research Article

Keywords: Aluminium, Nanoparticle, Pseudomonas, Biofilm, Humic Acids, Zinc oxide

Posted Date: August 31st, 2021

DOI: https://doi.org/10.21203/rs.3.rs-845701/v1

Version of Record: A version of this preprint was published at Microbial Ecology on January 23rd, 2022.
See the published version at https://doi.org/10.1007/s00248-022-01961-6.

Abstract

The use of metal-based and, particularly, Al_2O_3 nanoparticles (Al_2O_3_NP) for diverse purposes is exponentially growing. However, the growth of such promissory market is not accompanied by a parallel extensive investigation related to the impact of this pollution on groundwater and biological systems. *Pseudomonas* species, ubiquitous, environmentally critical microbes, frequently respond to stress conditions with diverse strategies that generally include extracellular polymeric substances (EPS) formation. The aim of this study is to report that changes in the aqueous environment, particularly, the addition of Al_2O_3-NP without and with humic acids, induce different adaptive strategies of *P. aeruginosa* early biofilms. To this purpose, early biofilms were incubated in diluted culture media without (control) and with Al_2O_3-NP, and with humic acids (HA-control, HA-Al_2O_3-NP) for 24h. 3D colonies with EPS strings and isolated bacteria in their surroundings were detected in the control biofilms. Unlikely, an unusual adaptive behaviour was developed in presence of Al_2O_3-NP. Bacteria opt to disassemble the 3D arrangements, and to implement a 2D network promoting morphological and size changes of bacterial cells (small coccoid shapes). Remarkably, this strategy allows their temporarily non-EPS-depending survival without decreasing the number of cells. This behaviour was not observed with ZnO-NP, HA-Al_2O_3-NP, or HA-ZnO-NP. Physicochemical analysis revealed that HA were adsorbed on Al_2O_3-NP and promoted the Al(III) ions complexation. This supports the hypothesis that the reduction of toxicity of Al ions and the 3D colony formation in presence of HA-Al_2O_3-NP is promoted by the complexation of the metal ions with HA components.

Introduction

Production of the engineered nanoparticles (NP) is growing exponentially due to their multiple applications. However, our understanding on the environmental fate and effects of these nanoproducts is far from being complete. There are several important factors to be considered in relation to groundwater contamination by NP, among them: release of metal ions by NP, surface reactions with organic components of aquatic media and NP impact in the biological environment [1]–[4]. Although most studies have been made considering the effect of high NP concentrations, latest investigations also report sublethal effects detected in some species over various generations [5].

Among metal oxide NPs, aluminium oxide NP (Al_2O_3-NP) are widely used. Considering the possible future expansion of this particular NP market, their impact under different natural exposure scenarios where Al-containing NP can accumulate deserves a special attention since they may affect biological ecosystems [5]–[7].

When the effects of NP disposal is investigated, the presence of dissolved organic matter and, particularly, humic acids (HA) should be taken into account [8] since they include –C = O, –COOH, –OH, –NH–, $–NH_2$, –N functional groups capable of interacting with NP and, in turn, conditioning the NP interaction with the microbial community.

Metal oxide NP are significant challenges for bacterial well-being since they may be toxic and create stress conditions such as pH and osmotic changes. Mature biofilms are generally more resistant to aggressive environments than the planktonic counterpart. Their resilience is frequently associated to the development of persisters (specialized survivor cells) able to survive to hard stress condition, and to the generation of the protective extracellular polymeric matrix (EPS) [9]. The EPS matrix is composed of DNA, bacterial polysaccharides, and proteins. Extracellular DNA (eDNA) is a highly anionic polymer that functions as a structural support to maintain biofilm structure. However, at specific concentrations, may cause cell lysis by chelating metal cations (such as Mg^{2+} and Ca^{2+}) that stabilize lipopolysaccharides and the outer membrane, inducing the release of the cytoplasmic content. [10], [11]

Pseudomonas species are ubiquitous, environmentally critical microbe able to employ many resistance mechanisms to survive in toxic environments and to thrive in human environments by biofilm development [11],[12]. In case of exposures to metal ions, the survival mechanisms do not seem to be similar to those for other toxic agents since, unlike antibiotics, both, planktonic and attached bacteria, may be tolerant to high concentrations of specific metal ions developing different strategies [13].

The aim of this work is to report an atypical adaptative strategy developed by *P. aeruginosa* early biofilms to survive in aqueous suspension of the widely used Al_2O_3-NP.

Materials And Methods

Materials

The assays with NP were made at 50 ppm concentration (subinhibitory concentration) using of commercially available Al_2O_3-NP (GetNanoMaterials, Purity: 99.97%) or ZnO-NP (GetNanoMaterials, purity:99.8). They were suspended in simulate natural waters inorganic matrix (SIM) (see experimental details in supporting information (SI)).

The different solutions/suspensions employed were: Control (SIM without NP); HA-Control (SIM with 10ppm of HA, without NP); NP (SIM with 50ppm NP in suspension: Al_2O_3-NP or ZnO-NP); HA-NP (SIM with 50ppm NP suspension with 10ppm of HA, HA-Al_2O_3-NP or HA-ZnO-NP).

Characterization assays and spectroscopic analysis:

Dynamic Light Scattering (DLS), FTIR-ATR spectroscopy analysis, and inductively coupled plasma (icp) atomic emission spectroscopy were used to physicochemical characterization of the NP and their suspensions (experimental details are included in SI).

Biofilm formation

Details of biofilms assays are described in SI following those previously reported with minor modifications [14], [15] [16]. Briefly, *Pseudomonas aeruginosa* (PAK wt) biofilms were formed during 1h in diluted culture medium (DCM) on sterilized glass slides and then were introduced into a multiwell plate

(24 wells) to form 24h-biofilms under different conditions: with 10 ppm HA, and 50 ppm of either a) Al_2O_3-NP or HA-Al_2O_3-NP; b) ZnO-NP or HA-ZnO-NP. The experiments were performed in duplicate, and the assays were repeated at least three times.

SEM microscopy

A scheme of biofilm formation like that described in the literature [17] with additional pretreatment to preserve biological material was used to perform SEM observations (see Supplementary Materials for details). EDS analysis was also performed (ESEM, FEI, Quanta 200 with EDX).

The analysis of the distribution of the lengths of the bacteria growing in biofilms was made using the images of SEM microscopy.

Results And Discussion

P. aeruginosa biofilm formation

Control. Initially early 1h-biofilms were formed on all glass samples after exposing the substrates to the planktonic culture in DCM. Epifluorescence microscopy (Figure S1) showed that isolated bacteria were attached on the surface and small microbial agglomerates were formed. The glass samples with the early biofilms were placed in a multiwell, the DCM was added, and the biofilm was following incubated for 24h. SEM observations (Fig. 1A, centre) showed that 3D colonies were formed on the control surface and the isolated bacteria were detected around the colonies (Fig. 1A (a)). Extracellular polymeric substances (EPS) can also be noticed in the microphotograph, EPS strings similar to those previously reported for other nanostructures [18] that connect bacteria and stick them to generate a 3D matrix can be identified (Fig. 1A, control (b) yellow arrows).

Al_2O_3-NP suspensions. Surprisingly, the addition of Al_2O_3-NP did not imply the reduction in the number of bacteria in relation to the control (Fig. 2A and 2B). However, SEM observations showed morphological changes of the rod-shape bacteria (Fig. 1B(b)) to coccoid and the reduction in the size (Fig. 2C), revealing a stress response to the toxic environment. Additionally, 3D colonies were not formed and a 2D bacterial net can be distinguished. Remarkably, bacteria were connected by flagella/nanotubes (Fig. 1B(b) blue arrows) that formed a biological meshwork without producing EPS. Considering that after the initial biofilm formation small microbial agglomerates were formed (Figure S1) and the surrounding bacteria were isolated without connections with the others, it can be inferred that during the subsequent 24h period, a peculiar restructuration occurred.

ZnO-NP suspensions. We wondered if bacterial nets were also formed in presence of other NP. Thus, similar experiments were performed in the presence of ZnO-NP, a widely used metal-based NP. In this case, the addition of 50 ppm ZnO-NP showed significantly higher living attached bacteria than the control (Fig. 1C, centre) but allocation of cells and distribution of sizes (Fig. 1C) were similar. Within the colonies, high amounts of EPS strings can be noticed (Fig. 1C(b), yellow arrows). In all cases nanotubes can be

distinguished, some of them are in the polar position and are probably flagella (blue arrows in Fig. 1C) while others seem to be generated to provide a connection between the bacterial cytoplasm.

Bacterial size and morphology

SEM microphotographs of attached bacteria allowed the statistical evaluation of bacterial sizes. It could be observed that in the presence of Al_2O_3-NP the attached bacteria were significantly smaller than those of the control (average lengths of 0.8μm and 1.4μm, respectively). The frequency distribution of the lengths (Fig. 2C) showed the marked influence of the environment both, in the bacterial size and morphology, the smaller sizes correspond to coccoid shapes. Conversely, in the presence of Zn-NP the bacterial size was larger, like that of the control. Thus, aluminium ions release by the Al_2O_3-NP may be a toxic agent for bacteria causing morphological and size changes in response to the stress condition. Consequently, considering that complexation of the cations may reduce the toxic effect and that the components of humic acids (HA, frequently present in natural aqueous environments) may function as chelator agents, we decided to add HA to the Al_2O_3-NP suspension and to investigate their influence in the physicochemical and biological response.

Physicochemical characterization.

Adsorption of humic acids. Figure S2 shows that the E465/E665 ratio in the liquid filtrate of a Al_2O_3-NP suspension containing HA is close to 3, indicating that the high molecular weight aromatic structures remain in the liquid filtrate and the low molecular weight aromatic compounds containing carboxylic and/or carbonyl groups are adsorbed on the Al_2O_3-NP surface. DLS results (Table S1) showed that the distribution of the diameters of the Al_2O_3-NP aggregates changes if HA is present.

FTIR-ATR results presented in Figure S3 complement this information (see SI for details). There, the spectra corresponding to HA, Al_2O_3-NP and the solid (HA-Al_2O_3-NP(s), Figure S3 left) and liquid phases (HA-Al_2O_3-NP(l), right) obtained by centrifugating the HA-Al_2O_3-NP suspensions are shown. Interestingly, the ATR-IR spectrum of HA-Al_2O_3-NP(s) showed the appearance of new important peaks at 3350 and 1620 cm^{-1}, characteristic of HO^- and COO^- vibrations, respectively, which were not observed for Al_2O_3-NP. The observed shift in the bands due to carboxylic groups on HA- Al_2O_3-NP (s) seems to support the formation of Al-carboxylic complexes on the Al_2O_3-NP surface, in line with E465/E665 results and literature reports [19]. On the other hand, in case of the liquid filtrate HA-Al_2O_3-NP(l) the shift of the band at 1586 cm^{-1} to 1637 cm^{-1} can be attributed to the carboxylate groups with covalent coordinated bonds formed when HA and Al(III) are present. Additionally, a shift from the 1090 cm^{-1} (HA) to 1114 and 1124 cm^{-1} for HA-$Al_2(SO_4)_3$ and HA-Al_2O_3-NP(l), respectively, also indicates the formation of coordination complexes between Al(III) and the organic aliphatic molecules with -OH groups.

Release of Al(III) ions. To determine the release of Al(III) by suspended Al_2O_3-NP, the concentration of Al-containing species in the liquid phase was evaluated. To that purpose, Al_2O_3-NP(l) was analysed by ICP.

The results showed that the Al-containing species released by Al_2O_3-NP in SIM suspensions was 0.993 ppm, while in the presence of HA (HA-Al_2O_3-NP(I)), the NP were able to release 2.77 ppm. Thus, these results are in accordance with FTIR-ATR findings supporting that the presence of HA favours the release of less toxic Al-carboxilic complexes.

Addition of HA-Al_2O_3-NP to the culture medium. The addition of HA-Al_2O_3-NP suspension to the bacterial culture medium resulted in the increase of the number of attached bacteria in relation to the control. SEM observations revealed that 3D colonies with EPS strings were formed and, consequently, HA addition probably led to the reduction of the stress by the chelation of Al-containing ions.

In HA-Al_2O_3-NP-containing medium isolated bacteria did not form a network. The average size was slightly larger with less coccoid shape bacteria than in the case of Al_2O_3-NP without HA but significantly smaller that the control (Fig. 1D, Fig. 2C).

As expected, the complexation of the Al ions by HA reduced the toxicity caused by these ions, however, the wellbeing growth condition not be achieved since their size is smaller.

In agreement, EDS analysis after the biofilm formation showed a decrease of Al/C ratio from 0.088 in presence of Al_2O_3-NP to 0.070 in presence of HA-Al_2O_3-NP, revealing a decrease of the relative Al content on the surface after the addition of these HA-containing NP due to the consequent complexation process.

Al_2O_3-NP toxicity and bacterial adaptive behaviour.

Pseudomonas species display different strategies to survive at high levels of Al ions. [21]. One of them is the generation of complexation agents where, among ligands of Al ions, citrate is a very good one [7]. Cellular changes are displayed and lead to a metabolic shift in order to convert malate to citrate to overcome the stress produced by high concentrations of Al ions [22]. It should also be considered that the resistance of *P. aeruginosa* biofilms decrease with time and they may be eradicated at similar ions concentrations than planktonic cells after 1 day exposure [23].

Results reported here show that in the case of *P. aeruginosa* transformations other than chemical can be produced since morphological and size changes of cells and architectural reforms of the biofilm take place. In fact, Fig. 2C shows bacterial size distributions for each condition and a sharp maximum close to 0.8 μm (corresponding to ca. 70% of the cells) can be seen for Al_2O_3-NP suspension while broad peaks in the 0.6–1.2 μm and in the 1.0-1.6 μm range are depicted for the HA-Al_2O_3-NP and HA-control conditions, highlighting the influence of the medium composition on the bacterial size distribution. Analogously, it has been reported that under stress conditions the morphology of these cells change to U shape and finally to coccoid bacteria probably by modifications in cell wall crosslink or metabolic activity. Morphological changes, motility and surface properties changes were also observed for media with sub-MIC antibiotics [24]. Atypical results are shown here for Al_2O_3-NP since they show that the original 3D

aggregates disappear and a 2D network is formed with nanotubes as connectors of small coccoid bacteria.

Nanotubes are intercellular connections between neighbouring bacteria when the surface density of some bacteria is low. It has been hypothesized that these nanotubes enable bacteria scavenge and deliver molecules inside them and represent an important form of bacterial communication in nature, providing a network for exchange of cellular molecules within and between species [25]. It was found that nanotubes mediate the transfer of cytoplasmic molecules between adjacent cells [26],[27]. Moreover, they may also enable transiently acquired nonhereditary resistance to antibiotics. Besides, the transference of plasmids also occurred granting hereditary features to recipient cells [28].

On the other hand, eDNA that may be produced through explosive cell lysis events could facilitate the survival in non-nutrient stress condition [29]. It was hypothesized that in unfavourable conditions weak bacterial cells die, and the survival cells live on their expense (strategy known as “bust-and-boom”) [30]. The detailed observation of Fig. 1B (left, red arrow) reveals that the direction of the nanotubes of several bacteria is focused on a particular cell that may act as a nutrient donor. Thus, bust-and-boom strategy may also be used by *P. aeruginosa* in the networks.

Notwithstanding that there is a persistent tendency in environmental literature to link toxicity with EPS formation our results show that, under the *in vitro* conditions analysed, EPS is not the way that *P. aeruginosa* use to adapt to the metal toxicity.

Conclusions

Results showed that changes in the aqueous environment, particularly, the addition of Al_2O_3-NP without and with HA, induce different adaptive strategies of *P. aeruginosa* early biofilms. Under the stress condition created by the presence of free Al ions released by the Al_2O_3-NP, early biofilms are restructured (Fig. 4). The initial small aggregates of bacteria disassemble, and a network is developed without EPS production. To the best of our knowledge this type of strategy has not been previously reported for *P. aeruginosa* associated to the presence of NP or Al ions.

During the meshwork generation, isolated bacteria joint with the neighbouring cells by using intercellular connections known as nanotubes that may be used to transport biological molecules, for bacterial communication and interaction, and for the network members to acquire nonhereditary resistance. This adaptive strategy leads to the reduction of the interactions with the toxic free Al-ions by restricting the contact of each cell with the environment to the nanotube-connectors.

2D network formation was associated to the presence of Al(III) free ions since it was observed neither with ZnO-NP nor when HA was added to the Al_2O_3-NP. In the case of HA-Al_2O_3-NP suspension, physicochemical results support the assumption of the adsorption of HA on Al_2O_3-NP and the complexation of metal ions with HA components that leads to the reduction of the toxicity. Under these

less toxic condition EPS is produced and 3D colonies are formed but the size of the bacteria growing with HA-Al_2O_3-NP, although larger than those obtained with Al_2O_3-NP, are smaller than that of the control cells, confirming that certain stress level persists. Remarkably, this strategy allows their temporarily non-EPS-dependent survival without decreasing the number of cells.

The atypical strategy reported here reveals the diverse mechanisms developed by bacteria to overcome stress conditions that should be considered for the design of the bioremediation processes and medical treatments for infections. Results contribute to the understanding of how bacteria cope with environmental changes that challenge survival, although further studies are being designed to achieve a detailed information about metabolic changes in different environmental conditions and exposure periods.

Declarations

Funding

D.R.S. thanks CONICET, Argentina, for their post-graduate studentships. M.C.G., M.F.L.M., and A.M. are research members of CONICET.

This work was supported by:

ANPCyT (grant numbers PICT 2015-1266, PICT 2016-1424, and PICT 2019-0631);

CONICET (grant numbers PIP 0601 and PUE 22920170100100CO) and

UNLP (grant number 11/X900).

Conflicts of interest/Competing interests (include appropriate disclosures)

The authors declare that they have no known competing financial interests or personal relationships that could have appeared to influence the work reported in this paper.

Availability of data and material (data transparency)

Data will be available for reviews and editors as required

Code availability (software application or custom code)

Not applicable

References

1. Gómez-Gómez B, Arregui L, Serrano S, Santos A, Pérez-Corona T, Madrid Y, “Unravelling mechanisms of bacterial quorum sensing disruption by metal-based nanoparticles,” Sci Total Environ, 696, 2019,

doi:10.1016/j.scitotenv.2019.133869

2. Meyer JS, Lyons-Darden T, Garman ER, Middleton ET, Schlekat CE (2020) Toxicity of Nanoparticulate Nickel to Aquatic Organisms: Review and Recommendations for Improvement of Toxicity Tests. Environ Toxicol Chem 39(10):1861–1883. doi:10.1002/etc.4812
3. Mertens J, Oorts K, Leverett D, Arijs K (2019) Effects of Silver Nitrate are a Conservative Estimate for the Effects of Silver Nanoparticles on Algae Growth and Daphnia magna Reproduction. Environ Toxicol Chem 38(8):1701–1713. doi:10.1002/etc.4463
4. Griffitt RJ, Luo J, Gao J, Bonzongo JC, Barber DS (2008) Effects of particle composition and species on toxicity of metallic nanomaterials in aquatic organisms. Environ Toxicol Chem 27(9):1972–1978. doi:10.1897/08-002.1
5. Doshi R, Braida W, Christodoulatos C, Wazne M, O'Connor G (2008) Nano-aluminum: Transport through sand columns and environmental effects on plants and soil communities. Environ Res 106(3):296–303. doi:10.1016/j.envres.2007.04.006
6. Nogueira DJ et al., "Crystalline phase-dependent toxicity of aluminum oxide nanoparticles toward Daphnia magna and ecological risk assessment," *Environ. Res.*, vol. 182, no. November 2019, 2020, doi: 10.1016/j.envres.2019.108987
7. Cardiano P et al (2017) Sequestration of Aluminium(III) by different natural and synthetic organic and inorganic ligands in aqueous solution. Chemosphere 186:535–545. doi:10.1016/j.chemosphere.2017.08.015
8. Bondareva L, Fedorova N, "The effect of humic substances on metal migration at the border of sediment and water flow," Environ Res, 190, no. March, 2020, doi:10.1016/j.envres.2020.109985
9. Harrison JJ, Ceri H, Turner RJ (2007) Multimetal resistance and tolerance in microbial biofilms. Nat Rev Microbiol 5(12):928–938. doi:10.1038/nrmicro1774
10. Mulcahy H, Charron-Mazenod L, Lewenza S (2010) Pseudomonas aeruginosa produces an extracellular deoxyribonuclease that is required for utilization of DNA as a nutrient source. Environ Microbiol 12(6):1621–1629. doi:10.1111/j.1462-2920.2010.02208.x
11. Mulcahy H, Charron-Mazenod L, Lewenza S (2008) Extracellular DNA chelates cations and induces antibiotic resistance in Pseudomonas aeruginosa biofilms. PLoS Pathog 4(11):1–13. doi:10.1371/journal.ppat.1000213
12. Cefalì E et al (2002) Morphologic variations in bacteria under stress conditions: Near-field optical studies. Scanning 24(6):274–283. doi:10.1002/sca.4950240601
13. Teitzel GM, Parsek MR (2003) Heavy metal resistance of biofilm and planktonic Pseudomonas aeruginosa. Appl Environ Microbiol 69(4):2313–2320. doi:10.1128/AEM.69.4.2313-2320.2003
14. Cendra MdelM, Blanco-Cabra N, Pedraz L, Torrents E (2019) Optimal environmental and culture conditions allow the in vitro coexistence of Pseudomonas aeruginosa and Staphylococcus aureus in stable biofilms. Sci Rep 9(1):1–17. doi:10.1038/s41598-019-52726-0
15. Favre-Bonté S, Köhler T, Van Delden C (2003) Biofilm formation by Pseudomonas aeruginosa: Role of the C4-HSL cell-to-cell signal and inhibition by azithromycin. J Antimicrob Chemother 52(4):598–

604. doi:10.1093/jac/dkg397

16. Bertuola M, Miñán A, Grillo CA, Cortizo MC, de Mele MAFL (2018) Corrosion protection of AZ31 alloy and constrained bacterial adhesion mediated by a polymeric coating obtained from a phytocompound. Colloids Surfaces B Biointerfaces 172:187–196
17. Powell LC et al., "Targeted disruption of the extracellular polymeric network of Pseudomonas aeruginosa biofilms by alginate oligosaccharides," npj Biofilms Microbiomes, 4, 1, 2018, doi:10.1038/s41522-018-0056-3
18. Rodríguez Sartori D, Bertuola M, Miñán A, Gonik E, Gonzalez MC, De Mele MFL (2021) Environmentally Induced Changes of Commercial Carbon Nanotubes in Aqueous Suspensions. Adaptive Behavior of Bacteria in Biofilms. ACS Omega 6(8):5197–5208. doi:10.1021/acsomega.0c05114
19. Barron AR (2014) The interaction of carboxylic acids with aluminium oxides: Journeying from a basic understanding of alumina nanoparticles to water treatment for industrial and humanitarian applications. Dalt Trans 43(22):8127–8143. doi:10.1039/c4dt00504j
20. Igbokwe IO, Igwenagu E, Igbokwe NA (2020) Aluminium toxicosis: A review of toxic actions and effects. Interdiscip Toxicol 12(2):45–70. doi:10.2478/intox-2019-0007
21. Appanna VD, Pierre MST, "Aluminum elicits exocellular phosphatidylethanolamine production in Pseudomonas fluorescens," *Appl. Environ. Microbiol.*, vol. 62, no. 8, pp. 2778–2782, 1996, doi: 10.1128/aem.62.8.2778-2782.1996
22. Mailloux RJ, Lemire J, Kalyuzhnyi S, Appanna V (2008) A novel metabolic network leads to enhanced citrate biogenesis in Pseudomonas fluorescens exposed to aluminum toxicity. Extremophiles 12(3):451–459. doi:10.1007/s00792-008-0150-1
23. Harrison JJ, Turner RJ, Ceri H (2005) Persister cells, the biofilm matrix and tolerance to metal cations in biofilm and planktonic Pseudomonas aeruginosa. Environ Microbiol 7(7):981–994. doi:10.1111/j.1462-2920.2005.00777.x
24. Monahan LG, Turnbull L, Osvath SR, Birch D, Charles IG, Whitchurch CB (2014) Rapid conversion of Pseudomonas aeruginosa to a spherical cell morphotype facilitates tolerance to carbapenems and penicillins but increases susceptibility to antimicrobial peptides. Antimicrob Agents Chemother 58(4):1956–1962. doi:10.1128/AAC.01901-13
25. Baidya AK, Bhattacharya S, Dubey GP, Mamou G, Ben-Yehuda S (2018) Bacterial nanotubes: a conduit for intercellular molecular trade. Curr Opin Microbiol 42:1–6. doi:10.1016/j.mib.2017.08.006
26. *bioRxiv*, no. 033, p. 2020.10.20.340307, 2020, [Online]. Available: http://biorxiv.org/content/early/2020/10/20/2020.10.20.340307.abstract
27. Cao Y, Jana S, Bowen L, Liu H, Jakubovics NS, Chen J (2020) Bacterial nanotubes mediate bacterial growth on periodic nano-pillars. Soft Matter 16(32):7613–7623. doi:10.1039/d0sm00602e
28. Dubey GP, Ben-Yehuda S (2011) Intercellular nanotubes mediate bacterial communication. Cell 144(4):590–600. doi:10.1016/j.cell.2011.01.015

29. Ivanković T et al (2020) Capillary bacterial migration on non-nutritive solid surfaces. Arh Hig Rada Toksikol 71(3):251–260. doi:10.2478/aiht-2020-71-3436
30. Bravo Z, Orruño M, Parada C, Kaberdin VR, Barcina I, Arana I (2016) The long-term survival of Acinetobacter baumannii ATCC 19606T under nutrient-deprived conditions does not require the entry into the viable but non-culturable state. Arch Microbiol 198:5. pp. 399–407. doi:10.1007/s00203-016-1200-1., “,”, no.

Figures

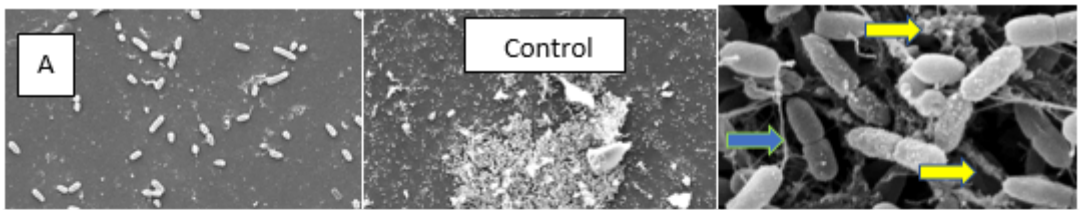

Figure 1

SEM microphotographs of early biofilms that were exposed for 24h to: (A) DCM (control), (B) the DCM + Al2O3-NP; (C) the DCM + ZnO-NP, (D) DCM + HA- Al2O3-NP. The figure in the centre correspond to the 2000X magnification while those on the left and on the right are details of the same sample at higher magnification. Yellow arrows point out EPS strings; blue arrows, the nanotubes and red arrows indicates that several nanotubes are directed to the same bacteria.

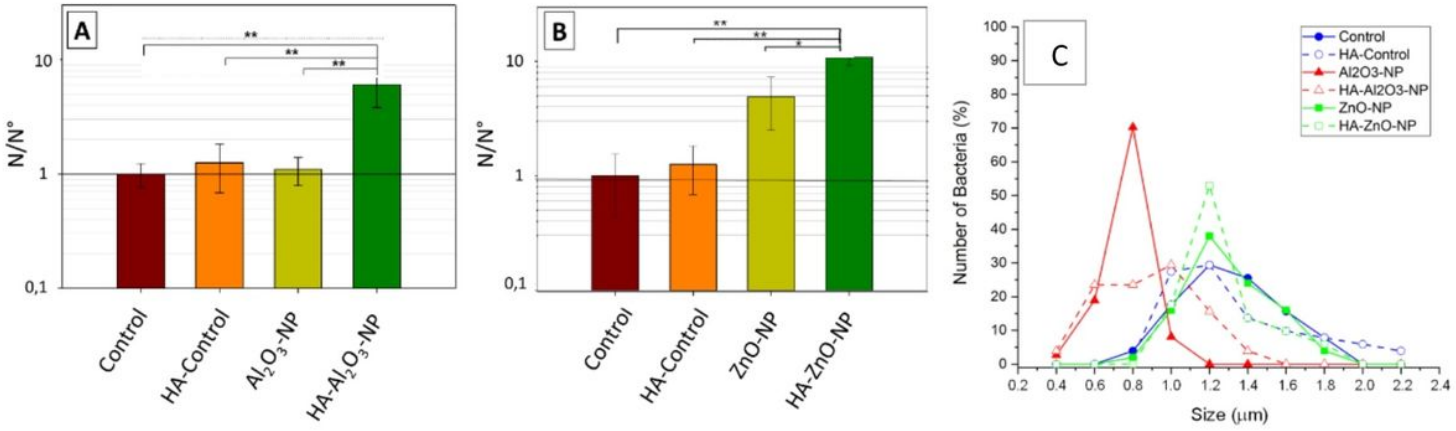

Figure 2

A and B: Enumeration of attached bacteria in the assays with and without NP The number of bacteria is normalized with respect to the control (N°). Control assays with and without HA are represented by the brown and orange columns respectively, the assays with the addition of Al2O3-NP or ZnO-NP are shown with light green and the HA-Al2O3-NP and HA-ZnO-NP assays with dark green columns. C: Percentage of bacteria of each size for the different conditions assayed: Control (blue solid line); Control + HA (blue dashed line); Al2O3-NP (red solid line); HA-Al2O3-NP (red dashed line); ZnO-NP (green solid line), and HA-ZnO-NP (green dashed line).

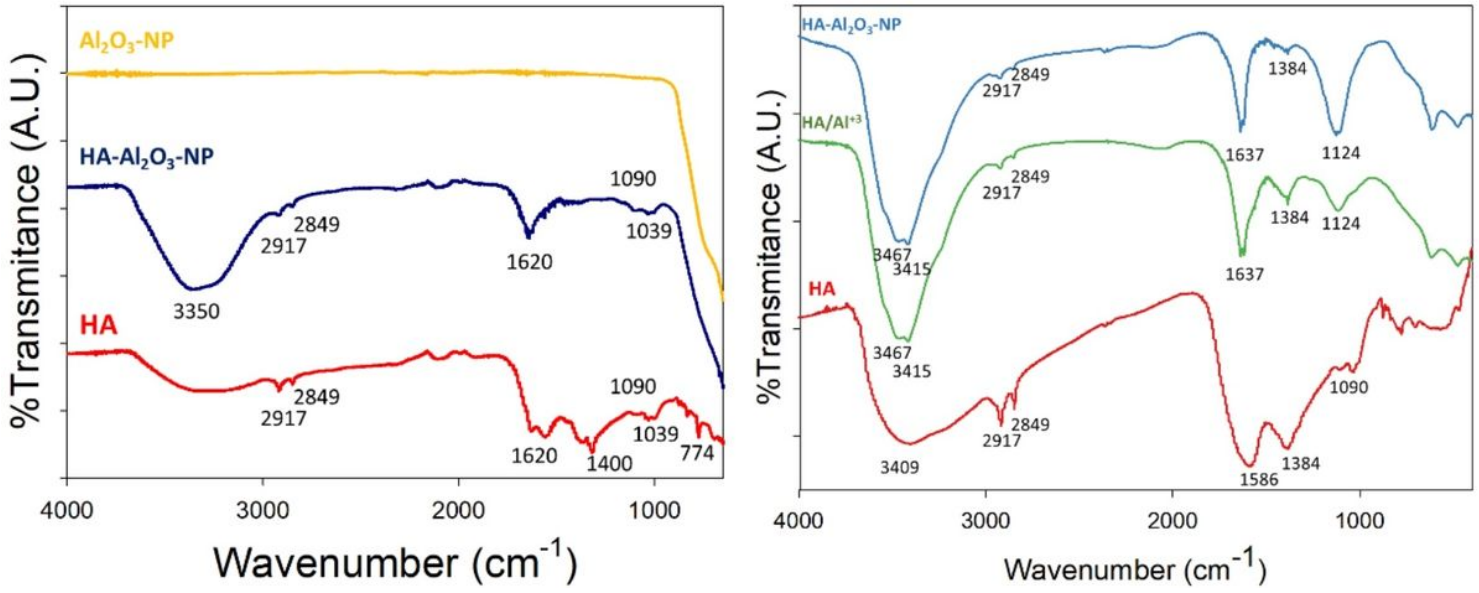

Figure 3

FTIR and ATR spectra. Left: ATR spectra obtained with Al2O3-NP solid phase (yellow), HA-Al2O3-NP solid phase after filtration (blue). Right: FTIR spectra obtained with HA + Al2(SO4)3 solution (green) and HA-Al2O3-NP liquid filtrate (light blue).

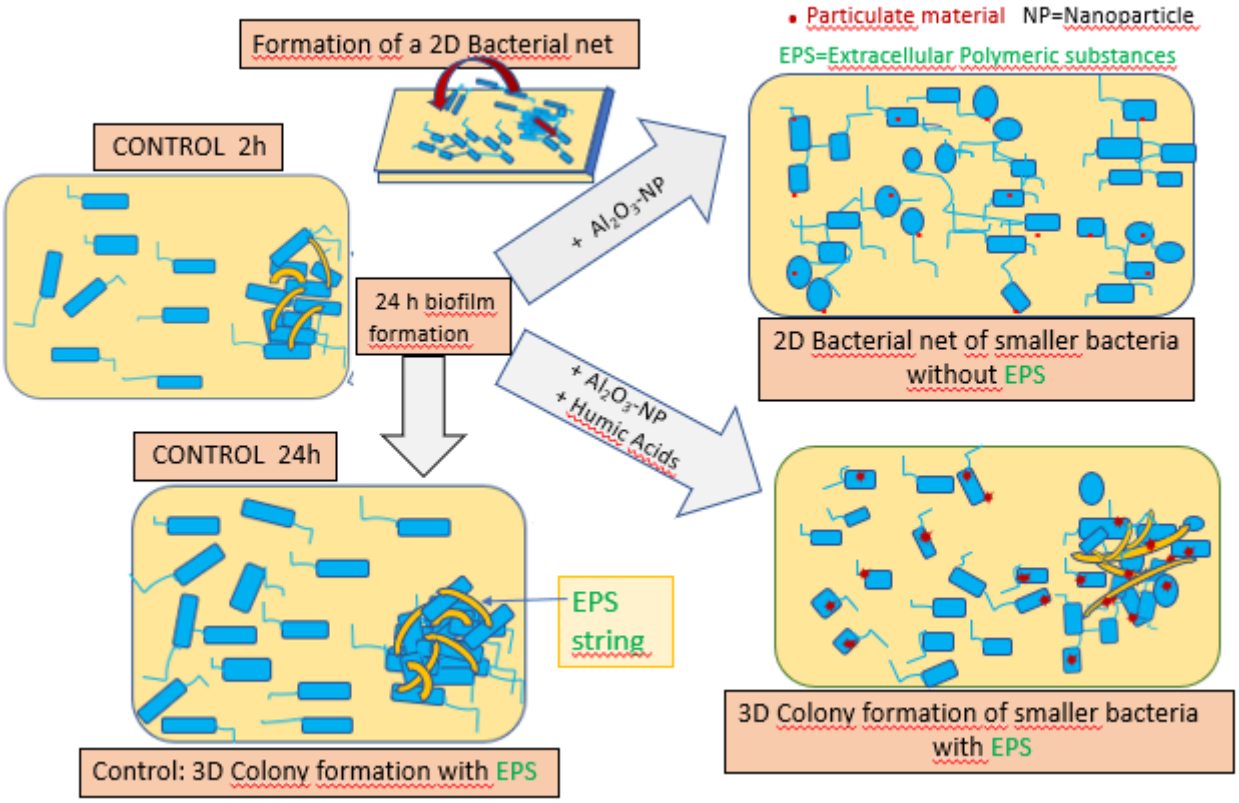

Figure 4

Scheme of the transformation of early biofilm architecture after being exposed for 24h to different media: culture medium (3D colony formation of normal rod-shape bacteria with EPS strings), Al2O3-NP suspension (network of smaller bacteria without EPS strings), and HA-Al2O3-NP (3D colony formation of smaller rod-shape and coccoid bacteria with EPS strings).

Supplementary Files

This is a list of supplementary files associated with this preprint. Click to download.

- SUPPLEMENTARYMATERIAL238.docx